Energy 358 (2026) 141350

Contents lists available at ScienceDirect

Energy

journal homepage: www.elsevier.com/locate/energy

Optimal district heating network expansion planning with resilience considerations☆

Jonathan Vieth *, Jan Westphal, Arne Speerforck

Institute of Engineering Thermodynamics, Hamburg University of Technology, Denickestraße 17, Hamburg, 21073, Germany

ARTICLE INFO

Keywords:
District heating network
District heating network planning
Optimization
Expansion planning
Resilience
Energy system planning

ABSTRACT

The use of carbon neutral heat sources such as industrial waste heat or large-scale heat pumps requires district heating networks. While automated planning of new district heating networks is well-studied, many metropolitan areas in Central Europe already have existing networks. The main challenge in metropolitan areas is to find the optimal district heating network expansion to connect new consumers to the already existing district heating network. The expansion may lead to overloading of existing pipes or generation units, which has to be considered in the planning process. For larger networks with multiple generation units, ensuring proper operation even during the failure of one generation unit is essential, making resilience a key factor in planning. In this work, we present an algorithm for automated and optimal expansion planning of district heating networks. The algorithm prevents overloads in existing and new pipes and incorporates potential outages of generation units to achieve a resilient network design. The approach was tested on a case study involving more than 3000 consumers and ten generation units with different price assumptions. Results show that the algorithm can compute an optimal expansion within 20 s, without considering resiliency. When considering resiliency, the computation time increases to 81 s or 876 s, depending on the price scenario. Furthermore, the peak demand added by the optimization decreases by up to 97 %. Therefore, considering resiliency has not only a major influence on expansion planning regarding the resulting topology, but also regarding computation time.

1. Introduction

For Germany to meet the targets of the European Green Deal, the heat supply of buildings must be decarbonized by 2050 [1]. A recent study showed that the share of buildings supplied with heat by district heating networks (DHNs) must increase to meet these targets [2]. The study analyzed four scenarios. In three of the four scenarios, the share of houses connected to DHNs in 2045 is at least double the share in 2020. These results align with those of [3], where the authors analyze for the country of Denmark, whether it reasonable to expand existing DHNs in Denmark from the perspectives of CO_2 reduction and cost.

DHNs already exist in most metropolitan areas in both Germany and Denmark. DHNs especially need to be expanded in urban areas because investment and operating costs decrease with increasing heat demand per unit area. Therefore, planning the expansion of existing DHNs is a major challenge.

1.1. Approaches to optimal district heating network planning

In general, two types of methodologies are common in the literature for optimally designing a new DHN. The first methodology uses graph techniques, while the second uses either mixed-integer-linear programming (MILP) or mixed-integer-nonlinear programming (MINLP) approaches.

1.1.1. Graph based approaches

Approaches for the automated generation of DHN simulation models based on OpenStreetMap (OSM) data are presented in [4,5]. Both use graph tools to determine the optimal topology from the set of possible routes defined by the OSM data. In [4], the optimal topology is approximated using shortest path searches, and in [5], it is approximated using Steiner tree algorithms. A Steiner tree is a subgraph of a graph that connects a subset of nodes, called terminal nodes, to each other such that the sum of the edge weights of the Steiner tree is smaller than the sum of the edge weights of any other tree that interconnects

☆ This article is part of a Special issue entitled: 'SDEWES 2025 - Invitation Only' published in Energy.

* Corresponding author.
E-mail addresses: jonathan.vieth@tuhh.de (J. Vieth), j.westphal@tuhh.de (J. Westphal), arne.speerforck@tuhh.de (A. Speerforck).

https://doi.org/10.1016/j.energy.2026.141350
Received 19 December 2025; Received in revised form 17 March 2026; Accepted 12 May 2026
Available online 20 May 2026
0360-5442/© 2026 The Authors. Published by Elsevier Ltd. This is an open access article under the CC BY license (http://creativecommons.org/licenses/by/4.0/).

Variables

$\dot{m}$	mass flow in $\mathrm{kg\,s^{-1}}$
$\dot{Q}$	heat demand in W
T	temperature in K
Δ	difference
c_w	specific heat capacity of water in $\mathrm{J\,kg^{-1}\,K^{-1}}$
$\mathcal{G}$	graph
$\mathcal{N}$	set of nodes of a graph
$\mathcal{E}$	set of edges of a graph
$\boldsymbol{A}$	incidence matrix of a graph
$\boldsymbol{C}$	matrix linking consumers to nodes
$\boldsymbol{G}$	matrix linking generation units to nodes
p	pressure in Pa
$\boldsymbol{U}$	matrix linking edges to pumps
$\boldsymbol{N}$	matrix linking edges to new edges
n	number of
ℓ	pipe length in m
λ	pipe friction factor
ρ	density of water in $\mathrm{kg\,m^{-3}}$
d	diameter in m
TPL	target pressure loss in $\mathrm{Pa\,m^{-1}}$
a	binary variable if edge is added to DHN
b	binary variable if consumer is added to DHN
c	specific cost parameter
C	total investment cost in €
R	reward from adding consumers to DHN in €
r	specific reward in $\mathrm{€\,kW^{-1}\,h^{-1}}$
Q	yearly heat demand of consumer in $\mathrm{kW\,h\,a^{-1}}$
A	annualized investment cost in $\mathrm{€\,a^{-1}}$
σ_{debt}	debt ratio
σ_{equity}	equity ratio
ψ	interest rate
ω	lifetime
J	objective function

Subscripts

max	maximum
pre	preexisting DHN edges
new	potentially new DHN edges
c	consumer
g	generation units
i	pipe intersections
pu	pump
pi	pipe
s	slack pressure required for new edges
nom	nominal values for pressure calculation
f	fail
st	street network

Abbreviations

DHN	district heating network
MIP	mixed-integer programming
MILP	mixed-integer-linear programming
MINLP	mixed-integer-nonlinear programming
OSM	OpenStreetMap
TPL	target pressure loss

all terminal nodes [6]. When using Steiner trees to find the optimal DHN topology, the terminal nodes are consumers and generation units. A more sophisticated method based on *price-collecting Steiner trees* is presented in [7], which uses the algorithm from [8]. When using price-collecting Steiner trees, not all terminal nodes must be part of the resulting DHN. The algorithm selects consumers worth adding to the DHN based on node attributes.

Graph-based approaches are typically fast and robust because they are derived from common graph theory problems. However, they only aim to find the shortest topology. The physics of the DHN, such as pressure and energy losses, are not considered during the topology search. For instance, in [9], all pipes that are part of the optimal topology are later dimensioned using a target pressure loss (TPL), as defined in [10].

1.1.2. Mixed-integer approaches

Conversely, MI(N)LP approaches can consider operational aspects in DHN design. Furthermore, these approaches can extend the system beyond classical DHNs by incorporating cooling networks, as presented in [11] or heat pumps at the consumer house stations, as presented in [12]. A good summary of several MI(N)LP approaches is given in [13].

Linear mixed-integer approaches. Résimont et al. [13] used a MILP for optimal DHN planning, where the DHN is represented using a linearized power flow approach based on the model presented in [14]. Similar to [7], a decision is made for each consumer within the region of interest as to whether the consumer should be connected to the DHN. Two use cases were considered. The larger use case contains 866 consumers and approximately 2000 streets, resulting in 35 111 design variables, and it took more than an hour to compute. Lambert et al. [15] present the DHN planning tool *topotherm* and compare it with four other optimal planning formulations, such as the one from [13]. Their results show that the MILP formulation from *topotherm* is the fastest due to its efficient representation of pipe operation direction. This representation uses two binary decision variables for pipe operation direction and one binary decision variable for building a pipe. In [16], a MILP approach is used to optimize the operation and design of a DHN simultaneously. Similar to the approach in [13], a power flow model is employed in which heat losses in the pipes are a linear function of the enthalpy flow entering each pipe. The methodology in [16] considers several time steps, not just the time step with the highest demand. This is reasonable because the efficiency of the heat pumps that supply a DHN depends on the source and supply temperatures, both of which are time dependent. However, this approach significantly increases the number of design variables because it considers the power flow variables of each pipe and time step during optimization. Therefore, [17] use clustering techniques to identify representative time periods throughout the year. The DHN is then optimized based on these time periods using *topotherm*.

Nonlinear mixed-integer approaches. In [18], a more accurate model than that presented in [13] is introduced, which takes the nonlinearity of the system into account. The steady-state model considers mass flows, pressures, and temperatures in the supply and return networks. It is of utmost importance to consider a nonlinear model since linear models will under- or overestimate losses in pipes, for example. If losses are underestimated, the resulting DHN may be infeasible. Conversely, if losses are overestimated, feasible solutions may be deemed unfeasible. However, the disadvantage of a nonlinear model is that it can only solve smaller case studies than in [13] in a reasonable amount of time. For example, solving the optimization problem for a case study with 160 consumers took 46 min. A mix of linear and nonlinear MIPs is used in [19]. First, a MILP algorithm is used to find the optimal DHN topology. Then, the optimal diameter of each pipe is calculated by solving a nonlinear thermo-hydraulic flow model. In [20], the authors were able to speed up the optimization in [18] by using a pipe diameter penalization strategy. The optimizer found an optimal topology and near-optimal pipe diameters in about 10 min. Another approach that considers multiple time steps is presented in [21]. In

Table 1
Comparison of mixed-integer optimization approaches regarding system size and model complexity. If more than one case study was used, the largest one regarding number of consumers was selected for this table.

Reference	MILP	MINLP	Number consumers	Number new consumers	Number producers	Uncertainty
Bordin et al. [28]	X		20	13	1	
Lambert et al. [29]	X		0[a]	47	4	X
Roland and Schmidt [30]		X	5	5	1	
Lerbinger et al. [31]	X		60	25	1	
Delangle et al. [32]	X		22	31	1	

[a] The used method is a multi-stage planning, hence the planning from e. g. second to third stage can be understood as an expansion planning.

this approach, a quasi-steady-state model of the DHN is used based on the work of [20]. Decoupling the time steps and solving them in parallel allows for efficient optimization. The results in [21] show that using several time steps leads to a lower overall system cost and better waste heat integration. In contrast to [21], Vieth et al. [9] use full-year dynamic simulations to incorporate various load cases into optimal DHN dimensioning. Here, the DHN models from [22] are used for simulating the DHN dynamically. The models are implemented in the dynamic programming language Modelica and were recently added to the TransiEnt library [23]. Another promising DHN simulation framework based on discrete event simulations was presented in [24].

1.2. Optimal district heating network retrofitting

None of the approaches discussed in Section 1.1 consider existing DHNs in the planning process. However, two recent works by Sollich et al. [25] and Tzouganakis et al. [26] consider existing DHNs for planning purposes. In [25], a nonlinear optimization approach is used to plan a new generation unit for an existing DHN. The goal is to transform the existing DHN into a 4th generation DHN, i. e., a DHN with a higher share of renewable energy sources and lower supply and return temperatures. For a formal definition of 4th generation DHNs, see [27]. Sollich et al. [25] used an accurate thermo-hydraulic model with multiple time-steps for the optimal generation unit planning. Generation units considered include gas boilers, heat pumps, solar thermal collectors, and electric boilers. The system with the lowest cost, consisting of operational and investment costs, is a combination of a heat pump and a gas or electric boiler, depending on the CO_2 price. However, a DHN expansion is not the focus of [25]. The first contribution of [26] is the validation of a simulation model for DHNs. This model was validated using an existing DHN, and the data was made publicly available, which greatly contributes to DHN research. Second, a genetic algorithm is used to calculate the optimal insulation material and thickness for the pipes. However, DHN expansion is not considered. Thus, [25,26] focus on improving the efficiency of existing DHNs, not expansion.

1.3. Optimal expansion planning

Table 1 collects optimization approaches that consider expanding an existing DHN by adding new consumers. Bordin et al. [28] used a MILP to plan the optimal expansion of a small, tree-shaped DHN with 20 consumers to include 13 new consumers. However, since the developed methodology does not allow for meshed preexisting DHNs, it is not applicable to large-scale DHNs, which are usually meshed. In contrast to [28,30] uses an accurate nonlinear model for optimal expansion planning of DHNs. However, as in [28], meshed existing DHNs are not permitted, and the number of consumers and generation units is small. Therefore, such a detailed optimization method is not applicable to large-scale DHNs. Lambert et al. [29] presented a *multi-stage optimization method* for DHN planning. Planning is performed in several stages and can be understood as expansion planning, although no preexisting DHN is considered. Uncertainty is considered in the form of heat demand and fuel prices. This is a very timely topic since long-term expansion planning must consider stochastic prices due to the uncertain development of fuel prices. However, Lambert et al. [29] validate the feasibility of their method using a small DHN with only 47 consumer nodes. Future work should test this methodology with large-scale DHNs. A sophisticated MILP optimization method for decarbonization planning in districts with a preexisting DHN is presented in [31]. In addition to the existing DHN, the study includes carbon capture and storage, as well as building retrofitting. However, the case study is small (60 buildings and one generation unit), and uncertainty is not considered. Delangle et al. [32] present another MILP approach. However, the case study is small, with only one generation unit and a small-scale DHN.

Apart from MI(N)LP approaches for the optimal DHN expansion, an expansion planning algorithm for meshed DHNs is presented in [33]. In [33], the simulation model from [34] is iteratively called within a multi-objective evolutionary algorithm. The result is a*Pareto front* that shows the trade-off between operating and investment costs. However, the case study only includes a few expansion routes. Therefore, it is questionable whether the presented multi-objective procedure is feasible for large-scale DHNs. Guelpa et al. [35] performed a feasibility study on the expansion of the very large DHN of Turin, which has around 5700 substations. The DHN is modeled using a fluid model; however, no optimal expansion is performed. Instead, several scenarios are tested using the model.

In summary, there are several different approaches to the design of DHNs. Some approaches use graph theory tools (e. g. [4,5,7]), others use nonlinear (e. g. [18]) or linear models (e. g. [16]). However, most of the literature focuses on the planning of *new* DHNs. Additionally, literature on DHN expansion planning uses small DHN examples with fewer than 100 consumers and often only one generation unit. Only Lambert et al. [29] consider uncertainty in DHN expansion planning by using stochastic prices and uncertainty regarding consumers' decisions to connect to the DHN. None of the aforementioned planning approaches consider resilience, despite it being an important concept in energy network planning. Resilience is considered in the planning process for energy hubs in [36]. Therefore, no physically modeled pipes were considered. In [37], resilience is assessed for integrated energy systems, including DHNs, by introducing resilience indices. Simulations are used to quantify the system's resilience using accurate dynamic models. However, no optimal planning is performed.

1.4. Contribution

This work presents a DHN expansion planning process that considers the resilience of the DHN. The objective is to determine the optimal set of routes and consumers to connect to the existing DHN from a set of possible routes and consumers. To consider resilience, the failure of a generation unit is ensured not to affect the DHN's heat supply. The algorithm is designed for planning large-scale DHNs in metropolitan areas. Since the decision in metropolitan areas is often not whether to expand the DHN, but where, the algorithm selects the consumers that will be most profitable for the DHN. A MILP approach was chosen for the planning process, since the focus are large-scale DHNs. To obtain a linear model, only the supply network's hydraulics are considered, along with linearized pressure losses.

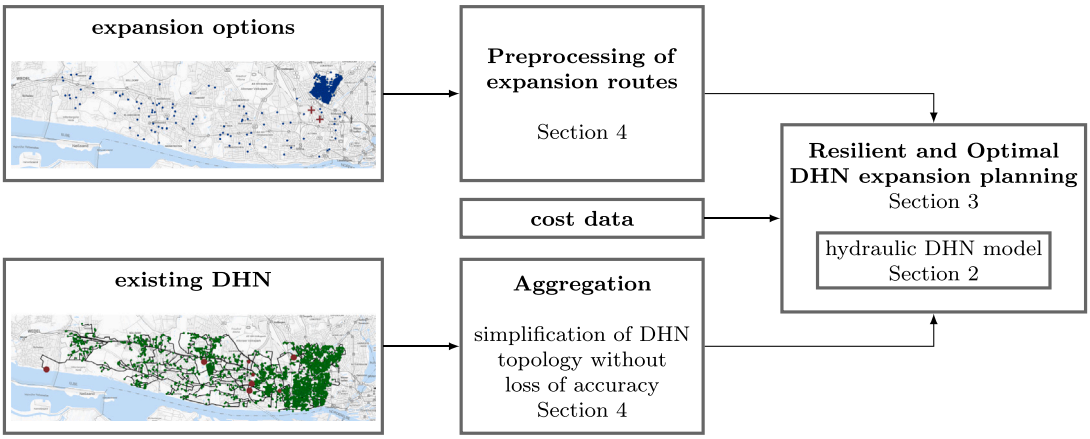

Fig. 1. Overview of the proposed method.

1.5. Structure

Fig. 1 provides an overview of the method presented in this paper. The structure of the paper is as follows: Section 2 presents the DHN model used. The DHN model is the core of the optimization process, the topic of Section 3. To speed up the optimization process, the DHN model and possible expansion routes are preprocessed. This approach is presented in Section 4. Section 5 applies the expansion planning method to a large-scale DHN with over 3000 consumers and ten generation units. The work concludes with a discussion of the expansion planning method and its results in Section 6, followed by a final conclusion including future work in Section 7.

2. District heating network model

As stated in the contribution, the goal of this work is to develop an expansion planning method for DHNs with resilience considerations. As pointed out in [20], there is always a trade-off between scalability and physical accuracy when developing DHN planning procedures. In conclusion, when planning the DHN of a metropolitan area and also considering the resilience of the system, a very scalable model is required. Hence, we propose a linear model that considers only the hydraulics of the supply network of the DHN. The DHN is divided into two parts. The first part is the existing DHN. The second part is all the possible routes that can be used to add the consumers to the DHN. For each consumer c that is part of the DHN or that is potentially added to the DHN, a maximum mass flow demand

$$\dot{m}^{c}_{\max} = \frac{\dot{Q}^{c}_{\max}}{c_{\mathrm{w}} \Delta T_{\mathrm{c}}} \tag{1a}$$

is calculated based on the maximum required heating power $\dot{Q}^{c}_{\max}$ of c, the specific heat capacity of water $c_{\mathrm{w}} = 4183\,\mathrm{J\,kg^{-1}\,K^{-1}}$, and a known supply and return temperature difference ΔT_{c} at the house station of c. The same approach is used to calculate the maximum mass flow generation

$$\dot{m}^{g}_{\max} = \frac{\dot{Q}^{g}_{\max}}{c_{\mathrm{w}} \Delta T_{\mathrm{g}}} \tag{1b}$$

of generation unit g with the supply and return temperature difference ΔT_{g} and maximum heat supply $\dot{Q}^{g}_{\max}$.

2.1. Graph representation

To model the DHN, the DHN is represented as a graph $\mathcal{G}(\mathcal{E}, \mathcal{N})$ similar to the approaches in [13,18]. Each edge $e \in \mathcal{E} = \mathcal{E}_{\mathrm{pre}} \cup \mathcal{E}_{\mathrm{new}}$ represents a pipe, where $\mathcal{E}_{\mathrm{pre}}$ is the set of edges that are part of the preexisting DHN and $\mathcal{E}_{\mathrm{new}}$ is the set of edges that can be added to the DHN in order to connect new consumers. Hence, the graph $\mathcal{G}_{\mathrm{pre}}(\mathcal{E}_{\mathrm{pre}}, \mathcal{N}_{\mathrm{pre}})$ represents the preexisting DHN, where $\mathcal{N}_{\mathrm{pre}}$ are the nodes in $\mathcal{G}$ that are connected to at least one edge in $\mathcal{E}_{\mathrm{pre}}$. The set of nodes $\mathcal{N} = \mathcal{N}^{\mathrm{c}} \cup \mathcal{N}^{\mathrm{g}} \cup \mathcal{N}^{\mathrm{i}}$ consists of the set of consumer nodes $\mathcal{N}^{\mathrm{c}}$, the set of generator nodes $\mathcal{N}^{\mathrm{g}}$, and the set of pipe intersections $\mathcal{N}^{\mathrm{i}}$. The set of consumer nodes $\mathcal{N}^{\mathrm{c}} = \mathcal{N}^{\mathrm{c}}_{\mathrm{pre}} \cup \mathcal{N}^{\mathrm{c}}_{\mathrm{new}}$ can be dissected into two sets: $\mathcal{N}^{\mathrm{c}}_{\mathrm{pre}}$, representing consumers that are connected to the preexisting DHN, and $\mathcal{N}^{\mathrm{c}}_{\mathrm{new}}$, representing potentially new consumers. The vector of mass flows $\dot{\boldsymbol{m}}^{\top} = \begin{bmatrix} \dot{\boldsymbol{m}}^{\top}_{\mathrm{pre}} & \dot{\boldsymbol{m}}^{\top}_{\mathrm{new}} \end{bmatrix}$ is decomposed into the mass flows $\dot{\boldsymbol{m}}^{\top}_{\mathrm{pre}} = \begin{bmatrix} \dot{m}^{1}_{\mathrm{pre}} & \dots & \dot{m}^{|\mathcal{E}_{\mathrm{pre}}|}_{\mathrm{pre}} \end{bmatrix}$ in the pipes of the preexisting DHN and $\dot{\boldsymbol{m}}^{\top}_{\mathrm{new}} = \begin{bmatrix} \dot{m}^{1}_{\mathrm{new}} & \dots & \dot{m}^{|\mathcal{E}_{\mathrm{new}}|}_{\mathrm{new}} \end{bmatrix}$ of potentially new pipes.

2.2. Constraints

At each node, the mass flow balance

$$\boldsymbol{A}\dot{\boldsymbol{m}} = \boldsymbol{C}\dot{\boldsymbol{m}}_{\mathrm{c}} - \boldsymbol{G}\dot{\boldsymbol{m}}_{\mathrm{g}} \tag{2a}$$

has to hold, where $\dot{\boldsymbol{m}}^{\top}_{\mathrm{g}} = \begin{bmatrix} \dot{m}^{1}_{\mathrm{g}} & \dots & \dot{m}^{|\mathcal{N}^{\mathrm{g}}|}_{\mathrm{g}} \end{bmatrix}$ is the mass flow generation, $\dot{\boldsymbol{m}}^{\top}_{\mathrm{c}} = \begin{bmatrix} \dot{m}^{1}_{\mathrm{c}} & \dots & \dot{m}^{|\mathcal{N}^{\mathrm{c}}|}_{\mathrm{c}} \end{bmatrix}$ is the mass flow consumption, $\boldsymbol{A}$ is the incidence matrix of $\mathcal{G}$, and $\boldsymbol{C}$ and $\boldsymbol{G}$ are matrices linking the consumers and the generation units to their respective nodes. For a formal definition of $\boldsymbol{A}$, see for example [38]. The vector of node pressures $\boldsymbol{p}^{\top} = \begin{bmatrix} p^{1} & \dots & p^{|\mathcal{N}|} \end{bmatrix}$ and the vector of pressure losses $\boldsymbol{\Delta p}^{\top} = \begin{bmatrix} \boldsymbol{\Delta p}^{\top}_{\mathrm{pre}} & \boldsymbol{\Delta p}^{\top}_{\mathrm{new}} \end{bmatrix}$ are linked by

$$\boldsymbol{A}^{\top}\boldsymbol{p} = \boldsymbol{\Delta p}(\dot{\boldsymbol{m}}) + \boldsymbol{U}\boldsymbol{\Delta p}_{\mathrm{pu}} + \boldsymbol{N}\boldsymbol{\Delta p}_{\mathrm{s}} \tag{2b}$$

with $\boldsymbol{\Delta p}^{\top}_{\mathrm{pu}} = \begin{bmatrix} \Delta p^{1}_{\mathrm{pu}} & \dots & \Delta p^{n_{\mathrm{pu}}}_{\mathrm{pu}} \end{bmatrix}$ the pressure differences introduced by the n_{pu} pumps, $\boldsymbol{U}$ is a matrix linking all edges of $\mathcal{G}$ to the edges that contain an additional pump, $\boldsymbol{N}$ is a matrix linking all edges of $\boldsymbol{G}$ to the potentially new edges, $\boldsymbol{\Delta p}^{\top}_{\mathrm{pre}} = \begin{bmatrix} \Delta p^{1}_{\mathrm{pre}} & \dots & \Delta p^{|\mathcal{E}_{\mathrm{pre}}|}_{\mathrm{pre}} \end{bmatrix}$ the pressure losses in the preexisting pipes, and $\boldsymbol{\Delta p}^{\top}_{\mathrm{new}} = \begin{bmatrix} \Delta p^{1}_{\mathrm{new}} & \dots & \Delta p^{|\mathcal{E}_{\mathrm{new}}|}_{\mathrm{new}} \end{bmatrix}$ the pressure losses in potentially new pipes. The vector of slack pressure differences $\boldsymbol{\Delta p}_{\mathrm{s}}$ is required for all new edges. If a potential edge e in between nodes n_1 and n_2 is not built, there is no direct relation between the pressure values p^{n_1} and p^{n_2}, hence the slack variable $\Delta p^{e}_{\mathrm{s}}$ is required. However, there is still a relation between p^{n_1} and p^{n_2} through other nodes. The vector of pressure losses is derived in the next section.

2.3. Pressure loss linearization

To derive a representation for $\boldsymbol{\Delta p}_{\mathrm{pre}}$, the preexisting DHN is exploited. A nominal mass flow $\dot{m}^{e}_{\mathrm{nom}}$ is already known in each pipe $e \in \mathcal{E}_{\mathrm{pre}}$ that is part of the preexisting DHN and is used for the

linearization. The nominal pressure loss $\Delta p^{\mathrm{pre}}_{\mathrm{nom}}$ can be calculated using the mass-flow-pressure-loss-correlation

$$\Delta p^e_{\mathrm{nom}} = \frac{8\ell_e \lambda_e}{\pi^2 \rho d_e^5} {\dot{m}^e_{\mathrm{nom}}}^2 \tag{3}$$

with the density of water $\rho = 983.19\,\mathrm{kg\,m^{-3}}$, the length ℓ_e, the friction factor λ_e, and the diameter d_e. Hence,

$$\Delta p^e_{\mathrm{pre}} = \frac{\Delta p^e_{\mathrm{nom}}}{\dot{m}^e_{\mathrm{nom}}} \dot{m}^e_{\mathrm{pre}}. \tag{4}$$

For each edge $e \in \mathcal{E}_{\mathrm{new}}$, a TPL TPL_e is used to calculate the pressure losses. Therefore, the pressure losses are given by

$$\Delta p^e_{\mathrm{new}} = \begin{cases} \ell_e \mathrm{TPL}_e \frac{|\dot{m}^e_{\mathrm{new}}|}{\dot{m}^e_{\mathrm{new}}}, & \dot{m}^e_{\mathrm{new}} \neq 0, \\ 0, & \text{otherwise.} \end{cases} \tag{5}$$

Note that using a TPL is a strong simplification, since the diameters are not optimally sized. However, it is not possible to find the optimal diameters using only hydraulics since heat losses are not explicitly modeled in the pipes. Heat losses are considered by the difference between ΔT_{g} and ΔT_{c}. However, even accurate optimization models that calculate pipe diameters optimally do not necessarily find the optimal diameters by using only the worst-case load situation, as shown in [21]. Furthermore, using dynamic DHN models as presented in [22,24] may reduce the optimal diameter further, since these models consider the heat capacity of the DHN. Hence, multiple time steps and dynamic thermo-hydraulic models are needed to find optimal pipe diameters. However, this is not in line with the goal of this work, which is to develop a model for large DHNs considering resiliency. Therefore, using a TPL is a reasonable simplification.

3. Optimal expansion planning with resilience considerations

This section deals with the optimal expansion planning of DHNs based on the DHN model derived in the previous section. To account for resilience, the failure of each $n_{\mathrm{f}} \leq n_{\mathrm{g}}$ generation unit is considered. Thus, (2) is solved n_{f} times. The more generation units that are allowed to fail during optimization, the more complicated the optimization problem becomes. Therefore, it might be reasonable to not consider the failure of all generation units, but rather only the n_{f} most risky ones (e. g. the largest ones).

First, the optimization variables are introduced and afterwards the objective and the constraints of the optimization problem are presented.

3.1. Optimization variables

Heendeniya et al. [39] framed the simultaneous consideration of energy system expansion and operational planning *co-planning*. Hence, it is reasonable to divide the variables into *expansion planning variables* and *operational planning variables*.

3.1.1. Expansion planning variables

For each edge $e \in \mathcal{E}_{\mathrm{new}}$, a binary variable a_e is required. If $a_e = 1$, edge e is added to the DHN, otherwise not. For each generation unit g, a maximum mass flow $\dot{m}^g_{\mathrm{max}}$ in the preexisting DHN is known. Since the hydraulic restrictions of the DHN may require an increase in generation, a vector of added mass flows $\Delta\dot{\boldsymbol{m}}_{\mathrm{g}}^{\top} = \begin{bmatrix} \Delta\dot{m}^1_{\mathrm{g}} & \dots & \Delta\dot{m}^{n_{\mathrm{g}}}_{\mathrm{g}} \end{bmatrix}$ at each generation unit is introduced. A binary variable b_c is introduced for each potential new consumer c, since the optimizer can select the most profitable consumers from an operational standpoint.

3.1.2. Operational planning variables

Individual hydraulic conditions of the DHN must be allowed for the failure of each generating unit. Hence, n_{f} mass flow vectors $\dot{\boldsymbol{m}}(f)$, node pressure vectors $\boldsymbol{p}(f)$, pump pressure vectors $\Delta\boldsymbol{p}_{\mathrm{pu}}(f)$, mass flow generation vectors $\dot{\boldsymbol{m}}_{\mathrm{g}}(f)$, and slack pressure vectors $\Delta\boldsymbol{p}_{\mathrm{s}}(f)$ are required, with $f \in \{1, \dots, n_{\mathrm{f}}\}$.

3.2. Objective

The main investment cost of the DHN is the cost of the pipes

$$C_{\mathrm{pi}} = c_{\mathrm{pi}} \sum_{e \in \mathcal{E}_{\mathrm{new}}} a_e \ell_e, \tag{6a}$$

where c_{pi} is the pipe cost per unit length. Second, the investment cost of the new generation units

$$C_{\mathrm{g}} = \sum_{g=1}^{n_{\mathrm{g}}} c_{\mathrm{g}} \left(\Delta\dot{m}^g_{\mathrm{g}} \right) \tag{6b}$$

has to be considered, where c_{g} maps the additional mass flows $\Delta\dot{m}^g_{\mathrm{g}}$ to investment costs. To select the best consumers from a DHN operator perspective, a reward function

$$R = r \sum_{c=1}^{|\mathcal{N}^{\mathrm{c}}_{\mathrm{new}}|} Q_c \tag{6c}$$

is used, with the yearly heat demand Q_c of the potentially new consumer c and r the reward per unit energy.

In order to compare the reward R of one year with the investment costs, C_{pi} and C_{g} are annualized using [40]

$$A_j = \sigma_{\mathrm{debt}} C_j \frac{\psi}{1 - (1+\psi)^{-\omega_j}} + \sigma_{\mathrm{equity}} \frac{C_j}{\omega_j}, \quad \forall j \in \{\mathrm{pi}, \mathrm{g}\}.$$

The debt and equity ratio are set to $\sigma_{\mathrm{debt}} = 0.29$ and $\sigma_{\mathrm{equity}} = 0.71$ [40] and the interest rate is set to $\psi = 0.04$ [12]. The lifetime ω_j depends on the matter of investment j and is 15 a for the generation units and 40 a for pipes.

The objective of the optimization is then given by

$$J = A_{\mathrm{pi}} + A_{\mathrm{g}} - R_{\mathrm{c}}. \tag{6d}$$

3.3. Constraints

Due to the binary variables $\boldsymbol{a}^{\top} = \begin{bmatrix} a_e & \dots & a_{|\mathcal{E}_{\mathrm{new}}|} \end{bmatrix}$, two additional constraints

$$\dot{m}^e_{\mathrm{new}} = 0, \quad \text{if } a_1 = 0, \quad \forall e \in \mathcal{E}_{\mathrm{new}}, \tag{7a}$$

$$\Delta p^e_{\mathrm{s}} = 0, \quad \text{if } a_e = 1, \quad \forall e \in \mathcal{E}_{\mathrm{new}} \tag{7b}$$

are required. Eq. (7a) is needed because a nonzero mass flow is allowed only in the case where edge e is added to the DHN, and (7b) because the slack pressure difference would falsify the results at added edges.

Eqs. (2) have to hold for the failure of each generation unit. Hence,

$$\boldsymbol{A}\dot{\boldsymbol{m}}(f) = \boldsymbol{G}\dot{\boldsymbol{m}}_{\mathrm{g}}(f) - \boldsymbol{C}\left(\begin{bmatrix} \mathbf{1}_{|\mathcal{N}^{\mathrm{c}}_{\mathrm{pre}}|} \\ \boldsymbol{b} \end{bmatrix} \circ \begin{bmatrix} \dot{\boldsymbol{m}}^{\mathrm{c}}_{\mathrm{pre}} \\ \dot{\boldsymbol{m}}^{\mathrm{c}}_{\mathrm{new}} \end{bmatrix} \right), \forall f \in \{1, \dots, n_{\mathrm{f}}\}, \tag{8a}$$

$$\boldsymbol{A}^{\top}\boldsymbol{p}(f) = \Delta\boldsymbol{p}(\dot{\boldsymbol{m}}(f)) + \boldsymbol{U}\Delta\boldsymbol{p}_{\mathrm{pu}}(f) + \boldsymbol{N}\Delta\boldsymbol{p}_{\mathrm{s}}(f), \forall f \in \{1, \dots, n_{\mathrm{f}}\}, \tag{8b}$$

where $\mathbf{1}_{|\mathcal{N}^{\mathrm{c}}_{\mathrm{pre}}|}$ is a vector with $|\mathcal{N}^{\mathrm{c}}_{\mathrm{pre}}|$ elements all equal to one and $\boldsymbol{b}^{\top} = \begin{bmatrix} b_1 & \dots & b_{|\mathcal{N}^{\mathrm{c}}_{\mathrm{new}}|} \end{bmatrix}$. In summary, if $b_c = 1$, the additional mass flow $\dot{m}^c_{\mathrm{new}}$ has to be met by the DHN at node n_c, where $\boldsymbol{C}$ links consumer c with node n_c. Due to the generation failure consideration, for each $f \in \{1, \dots, n_{\mathrm{f}}\}$ at one generation unit g no mass flow generation is allowed, which is described by

$$\dot{m}^g_{\mathrm{g}}(f) = 0. \tag{9}$$

The pressure values at all nodes have to be constrained in order to guarantee a safe operation of the DHN. This is achieved by adding the constraints

$$\boldsymbol{p}_{\mathrm{min}} \leq \boldsymbol{p}(f) \leq \boldsymbol{p}_{\mathrm{max}} \tag{10}$$

with $\boldsymbol{p}_{\mathrm{min}}$ and $\boldsymbol{p}_{\mathrm{max}}$ the vectors of minimum and maximum pressure values at the nodes. Furthermore, the maximum mass flow of the generation units

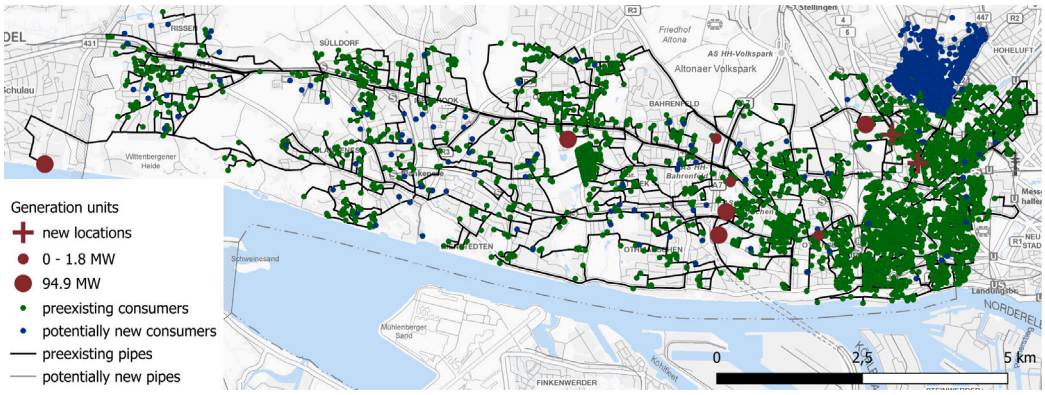

Fig. 2. Preexisting DHN and expansion options displayed on a map taken from [41].

$$\mathbf{0} = \dot{\boldsymbol{m}}_{\mathrm{g}}(f) \leq \dot{\boldsymbol{m}}^{\mathrm{g}}_{\max} + \boldsymbol{\Delta}\dot{\boldsymbol{m}}_{\mathrm{g}} \tag{11}$$

has to be respected by the optimization with $\dot{\boldsymbol{m}}^{\mathrm{g}}_{\max} = \begin{bmatrix} \dot{m}^{1}_{\max} & \dots & \dot{m}^{n_{\mathrm{g}}}_{\max} \end{bmatrix}^{\top}$.

4. Data preprocessing

The aim of this work is to find the optimal expansion planning of existing DHNs. To use this approach for large-scale DHNs in metropolitan areas with reasonable computation time of less than an hour, the data is preprocessed to reduce the number of optimization variables. The preprocessing consists of two steps:

1. Aggregation of the existing DHN
2. Reducing the number of graph edges for expansion planning

4.1. Aggregation of the existing network

The graph $\mathcal{G}_{\mathrm{pre}}$ representing the preexisting DHN is simplified to improve the computation time of the optimization. None of the simplifications performed have a negative impact on the accuracy of the model. The simplifications are based on the work of [42]. In a first step, all serial edges of $\mathcal{G}_{\mathrm{pre}}$ are aggregated to a single edge. Two edges e_1 and e_2 are called *serial edges* if both edges are connected to node n and the degree of n is two. This results in removing n from $\mathcal{G}_{\mathrm{pre}}$. However, n is removed only if there is no consumer or generation unit located at n.

Next, all edges are removed where the mass flow cannot be altered by the optimization. This includes all edges that are

- not in a loop or
- not part of a path in between two nodes with generation units.

This is achieved by finding all leaf nodes, i. e. nodes with a degree of one. Then all leaf nodes are deleted if there is no generation unit at the node. If a consumer is located at leaf node l with neighboring node n, the mass flow demand $\dot{m}^{l}_{\mathrm{c}}$ is added to $\dot{m}^{n}_{\mathrm{c}}$. Furthermore, the pressure loss in edge e connecting l to n is calculated and added to the minimum pressure at n. The pressure difference is calculated using (3) with the known maximum mass flow $\dot{m}_e$ in edge e. Note, that this simplification actually improves the accuracy of the model, since the physically correct mass-flow-pressure-loss relation (3) is used in all removed edges. The nodes neighboring potentially new consumers are not altered.

4.2. Possible routes for expansion

In [43], an algorithm is presented for finding the Steiner tree of a graph. The first step of this algorithm is to find the shortest path between each pair of terminal nodes. These are the only paths that can be part of the Steiner tree. This approach is similar to that presented in [44] for finding Steiner trees. In this work, the same approach is used to reduce the number of new edges in $\mathcal{G}$. The starting point is a graph $\mathcal{G}_{\mathrm{st}}\left(\mathcal{E}_{\mathrm{st}}, \mathcal{N}_{\mathrm{st}}\right)$ that represents the street network in between the potentially new consumers and the existing DHN. For each potentially new consumer c there is a node n_c in the set of nodes $\mathcal{N}^{\mathrm{c}}_{\mathrm{st}} \subseteq \mathcal{N}_{\mathrm{st}}$. Furthermore, a set of nodes $\mathcal{N}^{\mathrm{pre}}_{\mathrm{st}}$ is required, which contains all nodes that are part of $\mathcal{G}_{\mathrm{st}}$ as well as $\mathcal{G}_{\mathrm{pre}}$. According to [43,44], all possible expansion routes of $\mathcal{G}_{\mathrm{pre}}$ in order to connect the nodes contained in $\mathcal{N}^{\mathrm{c}}_{\mathrm{st}}$ are alongside the nodes $\mathcal{N}_{\mathrm{pre}} \subset \mathcal{N}_{\mathrm{st}}$ that are part of any shortest path in between two nodes $n_1, n_2 \in \mathcal{N}^{\mathrm{c}}_{\mathrm{st}} \cup \mathcal{N}^{\mathrm{pre}}_{\mathrm{st}}$.

5. Case study

The case study consists of a meshed preexisting DHN with 3187 consumers and $n_{\mathrm{g}} = 10$ generation units. Eight of the generation units are present in the preexisting DHN, and two are optional new generation unit locations. The goal is to determine the optimal expansion of the DHN in order to incorporate the most beneficial of the 610 potentially new consumers, while considering the possibility of failure of one of the five largest generation units, each with a maximum heating power of 94.9 MW. Fig. 2 depicts the preexisting DHN, the expansion options, the generation units, the preexisting consumers, and the new consumers. Most of the potentially new consumers are in the northeast of the existing DHN, while single consumers are scattered throughout the area already supplied by the DHN.

5.1. Input data

Only open-source data was used to create the preexisting DHN. This section discusses the generation of the preexisting DHN.

5.1.1. Consumer and generation data

All consumers selected for the existing DHN are located in areas that are actually supplied by a DHN. Information on DHN areas is taken from Zensus data. Following the approach in [9], yearly demand data and maximum heating power are obtained from a heat cadastre. The heat cadastre used is based on the work of [45]. All eight generation units that are part of the existing DHN are actual generation unit locations. However, for this case study, the maximum heating power was adapted.

Since the optimization uses a hydraulic DHN model, the heating power and demand must be converted to mass flows using (1). It is assumed that there is a temperature difference of $\Delta T_{\mathrm{g}} = 35\,\mathrm{K}$ at the generation units and a temperature difference of $\Delta T_{\mathrm{c}} = 30\,\mathrm{K}$ at the consumers. The total mass flow demand of all consumers in the preexisting DHN is $2590.88\,\mathrm{kg\,s^{-1}}$, and the total maximum mass flow of all generation units is $3258.8\,\mathrm{kg\,s^{-1}}$. The five largest generation units have a maximum mass flow of $647.97\,\mathrm{kg\,s^{-1}}$. Hence, even if the largest generation unit fails, the demand can be met by the other generation units. The DHN must deliver an additional mass flow of $688.86\,\mathrm{kg\,s^{-1}}$, to meet the demand of all possibly new consumers.

Table 2
Cost of additional generation units depending on $\Delta\dot{m}_g$ calculated from maximum additional heating power $\Delta\dot{Q}_g$ using (1) [47].

c_g in €	$\Delta\dot{m}_g$ in kg s^{-1}	$\Delta\dot{Q}_g$ in MW
1 792 000	13.65	2
4 210 000	34.13	5
8 040 000	68.25	10

5.1.2. Network data

The case study is based on the western section of the largest DHN in Hamburg, Germany. However, since real data is unavailable, the DHN topology was created using OSM data, accessed using the tools described in [46], and the shortest path search first presented in [4] and analyzed in [9], since it converges within seconds for a large DHN as considered in this work. In addition, one pipe was added manually to create the large mesh occupying nearly the whole DHN area, since large scale DHNs are usually meshed in order to guarantee save operation. The pipe inner diameters range from 0.0165 m to 0.73 m and were calculated using mass flows obtained from simulations and a TPL of 80 Pa m^{-1}, which is relatively low but still within the typical range. See [10] for more information on TPLes. In addition to the pumps at the generation units, there are nine more pumps throughout the DHN that are required to fulfill the minimum and maximum node pressures.

In summary, the locations of consumers and generation units represent a real DHN, while the piping network interconnecting them is artificial. Therefore, although the DHN is not real, it is as close as possible to a real DHN and is considered representative of a large-scale DHN in metropolitan areas.

5.2. Parameters

This section presents the parameters of the optimization presented in Section 3, including the choice of optimization algorithm.

5.2.1. Objective

For the investment cost data, $c_{pi} = 3000\,€\,m^{-1}$ is assumed, which is high in comparison to the data for example provided in [47]. However, in metropolitan areas, where large scale DHNs are usually present, investment cost of pipes is usually higher. For the additional generation units, the cost data is condensed in Table 2.

5.2.2. Constraints

In the planning process, it is assumed that the maximum pressure at each node is 25×10^5 Pa [48] and the minimum pressure is 5×10^5 Pa.

5.2.3. Solver

The resilient DHN expansion procedure was implemented in Python using Gurobi 12 as the optimization toolbox with an optimality gap of 2.5 % and the MIP focus parameter set to 3 in order to focus on the bound of the solution [49]. Otherwise the default setting were used.

5.3. Results of the preprocessing

Both the graph representing the preexisting DHN and the graph representing the expansion options were simplified based on the methods presented in Section 4. The results are provided below.

5.3.1. Aggregation of the existing network

Before aggregation, the graph modeling the preexisting DHN consisted of 18 091 edges and 18 091 nodes. The aggregation was able to decrease the number of nodes to 5761 and the number of edges to 5761 without reducing the accuracy of the model, as pointed out in Section 4.1. The number of edges and nodes is equal, since the graph has exactly one mesh (often called *cycle* in graph theory). Fig. 5 depicts the aggregated DHN together with the possible expansion routes.

Table 3
Comparison of the optimization results for resilient and non-resilient case and two price scenarios.

	Non-resilient		Resilient	
r in $\frac{€}{kW\ h}$	0.03	0.05	0.03	0.05
added demand in $\frac{kg}{s}$	644.582	667.825	19.959	563.95
added piping length in km	14.635	16.952	0.189	10.527
added generation in $\frac{kg}{s}$	0	0	0	544
calculation time in s	20.34	19.14	81.24	875.77

5.3.2. Possible routes for expansion

The graph containing potentially new edges is made up of 2602 nodes and 2432 edges, and is not connected because several consumers are spread out over the entire DHN area. Additionally, the graph contains 40 cycles.

5.4. Optimization results

To evaluate the expansion planning approach presented in Section 3, four scenarios were evaluated that varied in consumer reward r and resiliency consideration in the optimization. The results of all scenarios are summarized in Table 3. As expected, as r increases, more consumer demand is added to the DHN, resulting in a greater required piping length. For the non-resilient cases, r has no influence on calculation time, and no additional generation units are required.

However, in the non-resilient case and the second reward scenario, r increased by almost 67 %, but the added demand only increased by 3.6 %. This is because connecting more consumers would require additional generation units. This would not be beneficial, as consumers with relatively high rewards and low additional piping lengths are already included in the added demand. Increasing the demand by 3.6 % requires increasing the total added piping length by 15.8 %. This can be seen in Fig. 3(a). Here, each potential new consumer is shown alongside the two most important values that influence the decision of whether or not to add the consumer to the DHN compared to other consumers:

- the length of the shortest path from the consumer to any node that is part of the preexisting DHN. This can be understood as the required piping length to add only this one consumer to the DHN.
- the yearly heating demand influencing the objective J via (6c).

Almost all consumers with a yearly heating demand $Q \geq 2\times10^5$ kW h are connected to the DHN by the optimizer when $r = 0.03\,€\,kW^{-1}\,h^{-1}$. Increasing r to $r = 0.05\,€\,kW^{-1}\,h^{-1}$ adds one consumer with a high Q but also a very high shortest path length (see Fig. 3(b) compared with Fig. 3(a)). Otherwise, most additionally added consumers have a yearly heating demand of around 1×10^5 kW h and a relatively low shortest path length. Note, that the required piping length that is required to add a set of consumers is not equal to their summed shortest path length since consumers may be located close to each other; therefore, adding a single pipe may be needed to connect several consumers.

Considering resiliency in the expansion planning with $r = 0.03\,€\,kW^{-1}\,h^{-1}$, only seven consumers are added to the DHN, with a total mass flow demand of 19.959 kg s^{-1}. All of the them have a yearly heating demand higher than 4×10^5 kW h, and all but one have a shortest path length smaller than 30 m; however, the one consumer with a higher shortest path length is the one with the highest yearly heating demand as depicted in Fig. 4(a). Furthermore, some of the edges required to connect this consumer are also required to connect a second consumer added to the DHN, as shown in Fig. 4(a). The optimizer does not add more consumers since additional generation units would be required. The DHN's maximum mass flow generation when considering resiliency is 2610.9 kg s^{-1}. Therefore, adding more consumers requires adding more generation units, which is not optimal if $r = 0.03\,€\,kW^{-1}\,h^{-1}$.

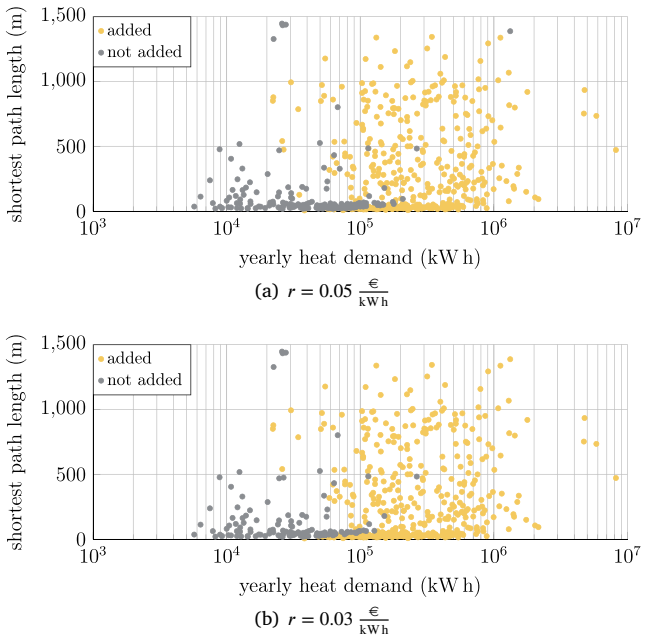

(a) $r = 0.05\ \frac{€}{\mathrm{kW\,h}}$

(b) $r = 0.03\ \frac{€}{\mathrm{kW\,h}}$

Fig. 3. Results of the optimal expansion planning without resiliency considerations.

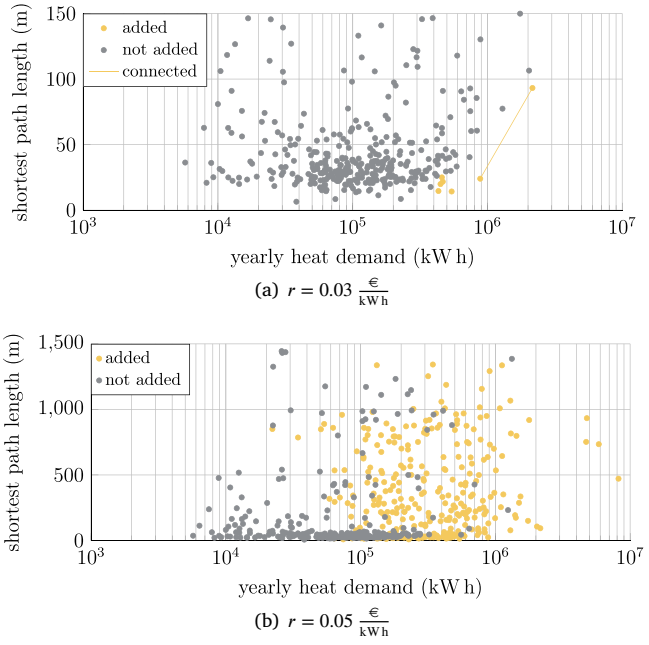

(a) $r = 0.03\ \frac{€}{\mathrm{kW\,h}}$

(b) $r = 0.05\ \frac{€}{\mathrm{kW\,h}}$

Fig. 4. Results of the optimal expansion planning considering resiliency.

However, when r is increased to $0.05\,€\,\mathrm{kW^{-1}\,h^{-1}}$, consumers with a total mass flow demand of $563.95\,\mathrm{kg\,s^{-1}}$ and generation units with a combined maximum mass flow of $544\,\mathrm{kg\,s^{-1}}$ are added. To add the new generation capacity, the optimizer also selected the two generation unit locations that were not present in the preexisting DHN, as shown in Fig. 5. In the resilient expansion planning scenario with $r = 0.05\,€\,\mathrm{kW^{-1}\,h^{-1}}$, the optimizer selects fewer consumers than in the non-resilient scenario with $r = 0.03\,€\,\mathrm{kW^{-1}\,h^{-1}}$. Nevertheless, the pattern of selecting consumers remains similar, as illustrated by comparing Fig. 3(a) with Fig. 4(b). Furthermore, the resilient and non-resilient optimizers focus on the northeastern part of the DHN, which has a high density of potentially new consumers (see Fig. 5). Zooming into this area (Fig. 6) reveals that the decision to add a consumer to the DHN depends heavily on the decision for neighboring consumers, in order to decrease the required piping length.

As expected, the resilient expansion planning took longer to converge to an optimal solution, since the number of variables is several times higher. For $r = 0.03\,€\,\mathrm{kW^{-1}\,h^{-1}}$, the optimizer solved the problem in 81.24 s, which is approximately four times longer than the calculation time for both non-resilient scenarios. However, for $r = 0.05\,€\,\mathrm{kW^{-1}\,h^{-1}}$, the optimization took 875.77 s. The increase in calculation time for $r = 0.05\,€\,\mathrm{kW^{-1}\,h^{-1}}$ may be due to the fact that for $r = 0.03\,€\,\mathrm{kW^{-1}\,h^{-1}}$, the solution space is much smaller since adding a generation unit is never optimal.

6. Discussion

This section discusses the proposed optimization method and the results of the case study.

6.1. Discussion of the results

As expected, consumers close to the existing DHN with high heating demands are preferred throughout all four scenarios (see Figs. 3 and 4). In the non-resilient scenario, the reward r has little influence on consumer connection (see Fig. 3). The existing DHN was designed to allow for the failure of any generation unit. Therefore, if the failure of any generation unit is not considered in expansion planning, the existing DHN is oversized in terms of generation units, and new consumers can be added without the need for additional generation units. In the resilient scenarios, however, almost no consumers are added in the lower reward scenario since additional generation units would be necessary. In the resilient scenario with a higher price, more consumers are added. However, this is still fewer than in the non-resilient scenario. The resilient scenario with the higher reward value is the only one with added generation units. Comparing Fig. 4(b) with Fig. 3(a) and 3(b) shows that consumers with similar properties regarding shortest path length and yearly heat demand are sometimes added and sometimes not in the resilient case. Other constraints, such as minimum pressure value and maximum mass flows, might play a more important role in this scenario than in the non-resilient scenarios.

6.2. Discussion and limits of the method

Other papers, such as [30], use more accurate DHN planning models, consider multiple time steps as in [21], or address DHN dynamics as in [9]. However, there is a lack of research on the expansion planning of large-scale DHNs. Furthermore, ensuring the resulting DHN's resilient operation is never considered. A linear approach, such as the one presented in this work, has several drawbacks. Since temperature is not considered and pressure losses are approximated using a linear model, the resulting DHN may be infeasible, or feasible solutions may be overlooked. Therefore, future work requires validating the results with an accurate nonlinear model, such as the dynamic models from [22]. Validation using dynamic simulation might show that the approach used in this work underestimates the resiliency of the DHN due to the inherent storage effects of a DHN. Another approach could be to add temperature optimization to hydraulic optimization, similar to the model predictive control approaches in [50] and in [51]. In [51], a thermo-hydraulic system is controlled optimally by performing a linear hydraulic optimization and a linear temperature optimization in a loop until convergence. This setup could also work for optimal DHN expansion planning.

A second limitation of the presented optimization is that uncertainties are insufficiently represented. Uncertainties that should be considered include prices, as discussed in [29], and malfunctions of

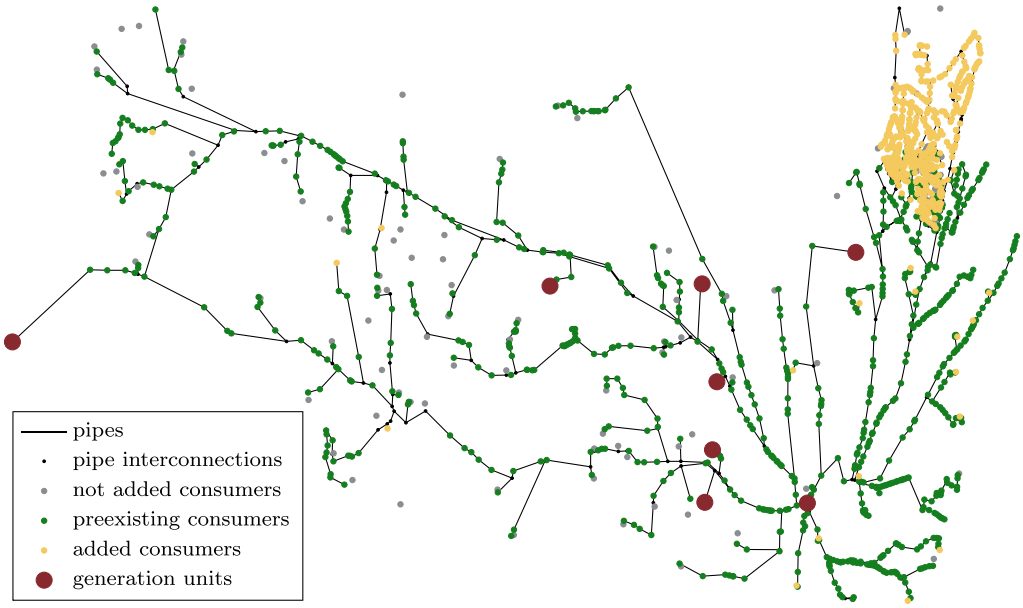

(a) Non-resilient

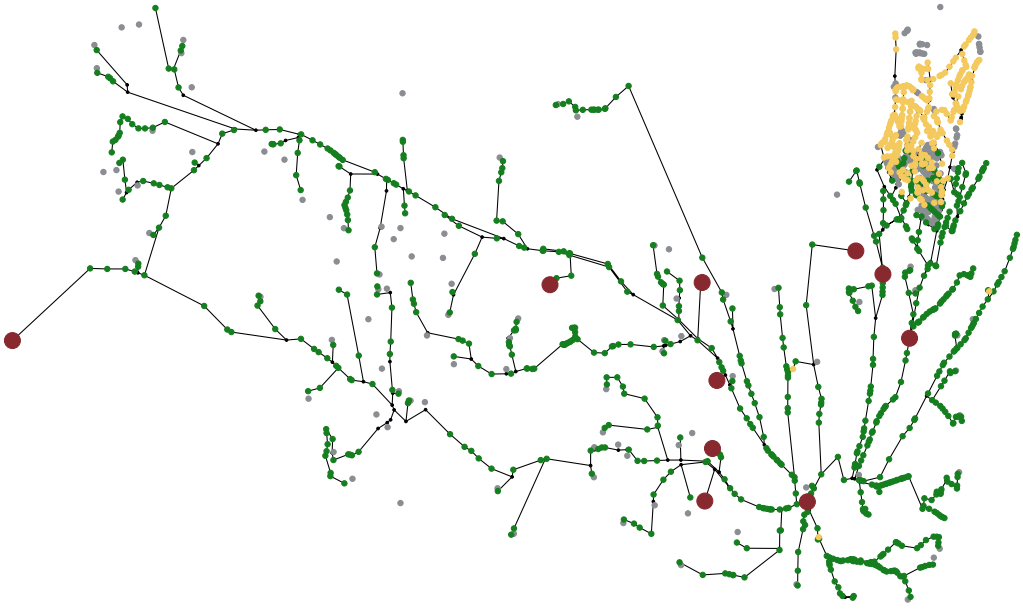

(b) Resilient

Fig. 5. Resulting DHN topology for $r = 0.05 \frac{€}{\mathrm{kWh}}$.

DHN components. This work only considers the malfunction of generation units and their associated pumps. However, problems such as pressure oscillations due to malfunction or poor control of consumer substations, as discussed in [52,53], are not considered. The same applies to controlling the temperature difference at substations. If some substations cannot reach the assumed temperature difference of 30 K, the resulting optimal DHN might be infeasible. In this case, a simulation with varying temperature differences after optimization or stochastic optimization is required. This, however, is left for future work, as is the validation of the approach using nonlinear models.

7. Conclusion and outlook

This work presents a methodology for resilient district heating network expansion. A resilient district heating network design is achieved by allowing for the failure of one generation unit. The district heating network is designed so that any generation unit can fail without disrupting the heat supply. Furthermore, the optimizer is able to select the best consumers from a set of possible consumers on its own resulting in a very profitable district heating network.

Since the methodology is aimed at large existing district heating networks and resilience has to be considered, a linear model is required that can deal with thousands of variables. This is achieved by considering the supply line of the district heating network, assuming fixed temperature differences at consumers and generation units.

The approach is tested with a case study consisting of an existing meshed district heating network with more than 3000 consumers, where the goal is to find the optimal district heating network expansion under varying price scenarios. The results show that considering resilience affects the optimal district heating network expansion massively. Furthermore, the presented approach is able to find the optimal

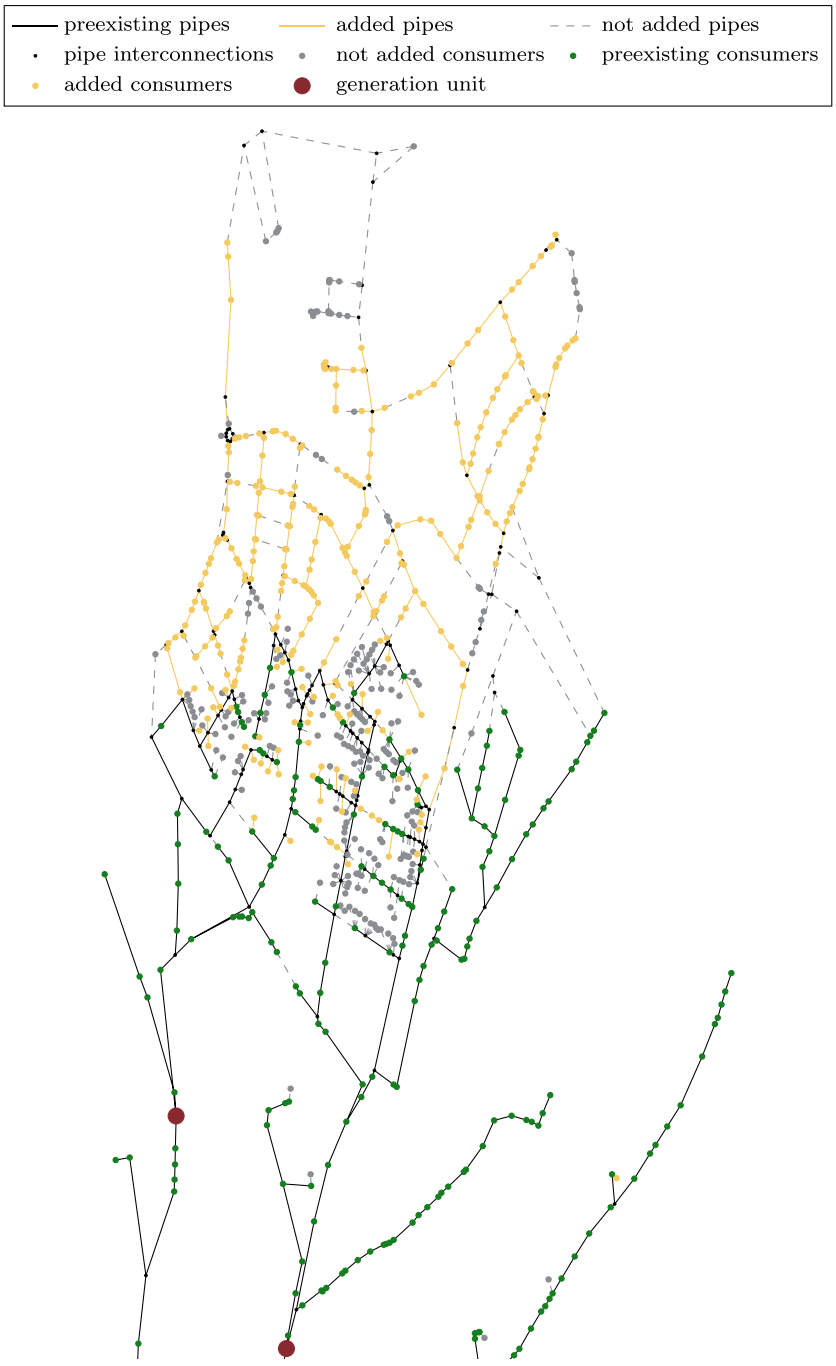

Fig. 6. Resilient expansion planing results with $r = 0.05\ \frac{€}{\mathrm{kWh}}$ in the north eastern area with a high density of potentially new consumers.

expansion within a reasonable time. Our approach has the potential of automating the district heating network planning in metropolitan areas, since it helps to identify areas of interest and creates the optimal expansion topology based on the provided data. District heating network operators can then use their own trusted tools to validate the results. We hope this will translate academic results into industry applications and greatly simplify district heating network planning in metropolitan areas.

Future research should incorporate temperature calculations alongside hydraulic optimization. Careful consideration must be given to balancing computation time and model accuracy to enable efficient planning of large-scale district heating networks. Furthermore, the resulting district heating network should be validated through dynamic simulations that account for various operational uncertainties inherent to large-scale systems. While this study focuses on optimal planning from the perspective of a district heating network operator, it would also be valuable to broaden the scope to a metropolitan area perspective by comparing district heating networks with other heating technologies, such as decentralized heat pumps.

CRediT authorship contribution statement

Jonathan Vieth: Writing – original draft, Visualization, Validation, Software, Methodology, Conceptualization. **Jan Westphal:** Writing – review & editing, Methodology. **Arne Speerforck:** Writing – review & editing, Supervision, Funding acquisition, Conceptualization.

Declaration of Generative AI and AI-assisted technologies in the writing process

During the preparation of this work, the authors used DeepL Write in order to improve language and readability. After using this tool, the authors reviewed and edited the content as needed and take full responsibility for the content of the published article.

Declaration of competing interest

The authors declare that they have no known competing financial interests or personal relationships that could have appeared to influence the work reported in this paper.

Acknowledgment

This research is supported by the German federal ministry of economic affairs and climate action (BMWK) under the agreement no. 03EWR007O2.

Data availability

Data will be made available on request.

References

[1] European Commission. The European green deal. Technical report, Brussels; 2019.
[2] Fraunhofer Institute for Solar Energy Systems. Wege zu einem klimaneutralen Energiesystem. Technical report, 2021.
[3] Lund H, Möller B, Mathiesen BV, Dyrelund A. The role of district heating in future renewable energy systems. Energy 2010;35(3):1381–90. http://dx.doi.org/10.1016/j.energy.2009.11.023.
[4] Fuchs M, Müller D. Automated design and model generation for a district heating network from OpenStreetMap data. In: Building simulation conference proceedings. IBPSA; 2017, http://dx.doi.org/10.26868/25222708.2017.562.
[5] Vieth J, Westphal J, Speerforck A. A GIS-based co-planning approach for district heating networks. 2024, http://dx.doi.org/10.46855/energy-proceedings-11423.
[6] Gilbert EN, Pollak HO. Steiner minimal trees. SIAM J Appl Math 1968;16(1):1–29. http://dx.doi.org/10.1137/0116001, Publisher: Society for Industrial and Applied Mathematics.
[7] Kuper L, Metzger M, Stursberg P, Niessen S. Computationally efficient topology design of district heating networks by price-collecting Steiner trees. Energy 2025;333:137223. http://dx.doi.org/10.1016/j.energy.2025.137223.
[8] Hegde C, Indyk P, Schmidt L. A nearly-linear time framework for graph-structured sparsity. 2015.
[9] Vieth J, Westphal J, Speerforck A. District heating network topology optimization and optimal co-planning using dynamic simulations. Adv Appl Energy 2025;19:100233. http://dx.doi.org/10.1016/j.adapen.2025.100233.
[10] Pirouti M, Bagdanavicius A, Ekanayake J, Wu J, Jenkins N. Energy consumption and economic analyses of a district heating network. Energy 2013;57:149–59. http://dx.doi.org/10.1016/j.energy.2013.01.065.
[11] Deng N, Cai R, Gao Y, Zhou Z, He G, Liu D, Zhang A. A MINLP model of optimal scheduling for a district heating and cooling system: A case study of an energy station in Tianjin. Energy 2017;141:1750–63. http://dx.doi.org/10.1016/j.energy.2017.10.130.
[12] Hering D, Xhonneux A, Müller D. Design optimization of a heating network with multiple heat pumps using mixed integer quadratically constrained programming. Energy 2021;226:120384. http://dx.doi.org/10.1016/j.energy.2021.120384.
[13] Résimont T, Louveaux Q, Dewallef P. Optimization tool for the strategic outline and sizing of district heating networks using a geographic information system. Energies 2021;14(17):5575. http://dx.doi.org/10.3390/en14175575, Publisher: Multidisciplinary Digital Publishing Institute.
[14] Sartor K, Quoilin S, Dewallef P. Simulation and optimization of a CHP biomass plant and district heating network. Appl Energy 2014;130:474–83. http://dx.doi.org/10.1016/j.apenergy.2014.01.097.
[15] Lambert J, Ceruti A, Spliethoff H. Benchmark of mixed-integer linear programming formulations for district heating network design. Energy 2024;308:132885. http://dx.doi.org/10.1016/j.energy.2024.132885.
[16] Haikarainen C, Pettersson F, Saxén H. A model for structural and operational optimization of distributed energy systems. Appl Therm Eng 2014;70(1):211–8. http://dx.doi.org/10.1016/j.applthermaleng.2014.04.049.
[17] Ceruti A, Lambert J, Spliethoff H. Integrating renewable energy and thermal storage in district heating networks: A design optimization approach. Energy Convers Manage 2025;345:120323. http://dx.doi.org/10.1016/j.enconman.2025.120323.
[18] Blommaert M, Wack Y, Baelmans M. An adjoint optimization approach for the topological design of large-scale district heating networks based on nonlinear models. Appl Energy 2020;280:116025. http://dx.doi.org/10.1016/j.apenergy.2020.116025.
[19] Lambert J, Spliethoff H. A two-phase nonlinear optimization method for routing and sizing district heating systems. Energy 2024. http://dx.doi.org/10.1016/j.energy.2024.131843.
[20] Wack Y, Baelmans M, Salenbien R, Blommaert M. Economic topology optimization of district heating networks using a pipe penalization approach. Energy 2023;264:126161. http://dx.doi.org/10.1016/j.energy.2022.126161.
[21] Wack Y, Sollich M, Salenbien R, Diriken J, Baelmans M, Blommaert M. A multi-period topology and design optimization approach for district heating networks. Appl Energy 2024;367:123380. http://dx.doi.org/10.1016/j.apenergy.2024.123380.
[22] Westphal J, Brunnemann J, Speerforck A. Enabling the dynamic simulation of an unaggregated, meshed district heating network with several thousand substations. Energy 2025;135434. http://dx.doi.org/10.1016/j.energy.2025.135434.
[23] Gillner M, Westphal J, Wiegel B, Steffen T, Urbansky J, Hagemeier A, Ruppert S, Heyer A, Benthin J, Hanke T, Brunnemann J, Becker C, Speerforck A. Status of the TransiEnt library: Transient simulation of complex integrated energy systems. Model Conf 2025;989–99. http://dx.doi.org/10.3384/ecp218989.
[24] Xie Z, Wang H, Hua P, Lahdelma R. Hydraulic-thermal dynamic model of meshed district heating network based on discrete event simulation. Energy 2025;339:138895. http://dx.doi.org/10.1016/j.energy.2025.138895.
[25] Sollich M, Wack Y, Salenbien R, Blommaert M. Decarbonization of existing heating networks through optimal producer retrofit and low-temperature operation. Appl Energy 2025;378:124796. http://dx.doi.org/10.1016/j.apenergy.2024.124796.
[26] Tzouganakis P, Fotopoulou M, Rakopoulos D, Romanchenko D, Nikolopoulos N. District heating system analysis and design optimization. Energy 2025;326:136349. http://dx.doi.org/10.1016/j.energy.2025.136349.
[27] Lund H, Werner S, Wiltshire R, Svendsen S, Thorsen JE, Hvelplund F, Mathiesen BV. 4Th generation district heating (4GDH): Integrating smart thermal grids into future sustainable energy systems. Energy 2014;68:1–11. http://dx.doi.org/10.1016/j.energy.2014.02.089.
[28] Bordin C, Gordini A, Vigo D. An optimization approach for district heating strategic network design. European J Oper Res 2016;252(1):296–307. http://dx.doi.org/10.1016/j.ejor.2015.12.049.
[29] Lambert RSC, Maier S, Shah N, Polak JW. Optimal phasing of district heating network investments using multi-stage stochastic programming. Int J Sustain Energy Plan Manag 2016;9:57–74. http://dx.doi.org/10.5278/ijsepm.2016.9.5.
[30] Roland M, Schmidt M. Mixed-integer nonlinear optimization for district heating network expansion. At - Autom 2020;68(12):985–1000. http://dx.doi.org/10.1515/auto-2020-0063.
[31] Lerbinger A, Petkov I, Mavromatidis G, Knoeri C. Optimal decarbonization strategies for existing districts considering energy systems and retrofits. Appl Energy 2023;352:121863. http://dx.doi.org/10.1016/j.apenergy.2023.121863.
[32] Delangle A, Lambert RSC, Shah N, Acha S, Markides CN. Modelling and optimising the marginal expansion of an existing district heating network. Energy 2017;140:209–23. http://dx.doi.org/10.1016/j.energy.2017.08.066.
[33] Vesterlund M, Toffolo A. Design optimization of a district heating network expansion, a case study for the town of Kiruna. Appl Sci 2017;7(5). http://dx.doi.org/10.3390/app7050488.
[34] Vesterlund M, Dahl J. A method for the simulation and optimization of district heating systems with meshed networks. Energy Convers Manage 2015;89:555–67. http://dx.doi.org/10.1016/j.enconman.2014.10.002.
[35] Guelpa E, Mutani G, Todeschi V, Verda V. A feasibility study on the potential expansion of the district heating network of Turin. Energy Procedia 2017;122:847–52. http://dx.doi.org/10.1016/j.egypro.2017.07.446.
[36] Rahgozar S, Zare Ghaleh Seyyedi A, Siano P. A resilience-oriented planning of energy hub by considering demand response program and energy storage systems. J Energy Storage 2022;52:104841. http://dx.doi.org/10.1016/j.est.2022.104841.
[37] Senkel A, Bode C, Schmitz G. Quantification of the resilience of integrated energy systems using dynamic simulation. Reliab Eng Syst Saf 2021;209:107447. http://dx.doi.org/10.15480/882.3263, Publisher: Elsevier Science.
[38] Desoer CA, Kuh ES. Basic circuit theory. New York: McGraw-Hill; 1969.
[39] Heendeniya CB, Sumper A, Eicker U. The multi-energy system co-planning of nearly zero-energy districts – Status-quo and future research potential. Appl Energy 2020;267:114953. http://dx.doi.org/10.1016/j.apenergy.2020.114953, Publisher: Elsevier BV.

[40] Oliva H. S, Garcia G. M. Investigating the impact of variable energy prices and renewable generation on the annualized cost of hydrogen. Int J Hydrog Energy 2023;48(37):13756–66. http://dx.doi.org/10.1016/j.ijhydene.2022.12.304.
[41] Landesbetrieb Geoinformation und Vermessung (LGV) Hamburg. WMS geobasiskarten hamburg (grau-blau). 2025, Data licence Germany – attribution – Version 2.0; https://metaver.de/trefferanzeige?docuuid=BE8E6014-60AD-4FD4-BE99-2FD8D75E0BDE. [Accessed 16 December 2025].
[42] Loewen A. Entwicklung eines verfahrens zur aggregation komplexer fernwärmenetze. In: UMSICHT-schriftenreihe, vol. 29, Stuttgart: Fraunhofer-IRB-Verl. 2001.
[43] Mehlhorn K. A faster approximation algorithm for the Steiner problem in graphs. Inform Process Lett 1988;27(3):125–8. http://dx.doi.org/10.1016/0020-0190(88)90066-X.
[44] Kou L, Markowsky G, Berman L. A fast algorithm for Steiner trees. Acta Inform 1981;15(2):141–5. http://dx.doi.org/10.1007/BF00288961, Publisher: Springer; Springer-Verlag.
[45] Dochev I, Seller H, Peters I. Assigning energetic archetypes to a digital cadastre and estimating building heat demand. An example from hamburg, Germany. Environ Clim Technol 2020;24(1):233–53. http://dx.doi.org/10.2478/rtuect-2020-0014.
[46] Boeing G. Modeling and analyzing urban networks and amenities with OSMnx. 2024.
[47] Langreder, Nora, Lettow, Frederik, Sahnoun, Malek, Kreidelmeyer, Sven, Wünsch, Aurel, Lengning, Saskia. Leitfaden Wärmeplanung. Technical Report, ifeu – Institut für Energie- und Umweltforschung Heidelberg and Öko-Institut e.V., IER Stuttgart, adelphi consult GmbH, Becker Büttner Held PartGmbB, Prognos AG; 2024.
[48] Hamburger Energiewerke. Unsere Netze. 2025, https://waerme.hamburger-energiewerke.de/netze-und-projekte/unsere-netze. [Accessed 22 April 2025].
[49] Gurobi Optimization LLC. Gurobi optimizer reference manual. 2025, https://docs.gurobi.com/projects/optimizer/en/12.0/index.html. [Accessed 17 December 2025].
[50] Li Z, Wu W, Shahidehpour M, Wang J, Zhang B. Combined heat and power dispatch considering pipeline energy storage of district heating network. IEEE Trans Sustain Energy 2016;7(1):12–22. http://dx.doi.org/10.1109/TSTE.2015.2467383.
[51] Vieth J, Eichler A, Speerforck A. Model predictive control of thermo-hydraulic systems using primal decomposition. 2026, http://dx.doi.org/10.48550/arXiv.2601.10189, arXiv:2601.10189 [eess]. This work has been accepted for presentation at the IFAC World Congress 2026.
[52] Lennermo G, Lauenburg P, Brand L. Decentralised heat supply in district heating systems : Implications of varying differential pressure. In: Proceedings from the 14th international symposium on district heating and cooling. SwedishDistrict Heating Association; 2014.
[53] Boysen H, Thorsen JE. How to avoid pressure oscillations in district heating systems. 2003.